Modeling of the Effects of Gaseous and Particulate Pollutants in the Urban Atmosphere. Part I: Thermal Structure

R. W. BERGSTROM, JR.,[1] AND R. VISKANTA

School of Mechanical Engineering, Purdue University, West Lafayette, Ind. 47907

(Manuscript received 6 March 1973, in revised form 6 June 1973)

ABSTRACT

The short-term effect of radiatively participating pollutants upon the temperature distribution in the boundary layer of the urban atmosphere is predicted. This is accomplished by constructing a mathematical model for atmospheric radiation transfer and one-dimensional mass, momentum and energy transport in the planetary boundary layer. The atmosphere, consisting of gaseous and particulate pollutants as well as natural constituents, is considered to absorb, emit and scatter anisotropically radiant energy. A series of numerical simulations of the thermal structure in the urban atmosphere is performed for summer and winter conditions, with and without an elevated inversion.

The numerical simulations showed that the aerosol pollutants reduced the solar radiant flux at the surface which in turn lowered its temperature during the day. The additional solar heating due to the pollutants caused the atmosphere to be slightly warmer at higher altitudes. The surface temperatures during the day were slightly higher for non-absorbing aerosols than for aerosols with some absorption. Under the conditions investigated the largest surface temperature reduction was 2C, and the maximum rise of the atmospheric temperature due to the additional solar heating was about 1C after a two-day period.

The gaseous pollutants increased the downward thermal radiation flux and thus raised the surface temperatures at night. The maximum predicted surface temperature increase was about 3C after a two-day simulation. The pollutant gases were shown to enhance the net radiative cooling below a stable region. This additional cooling modified both the nighttime stable layer and the elevated inversion by causing an upward motion of the stable regions. Thus, radiatively participating pollutants were shown to have the potential for changing the thermal structure of an urban atmosphere.

1. Introduction

In addition to being a health hazard, air pollution has been considered by many atmospheric scientists to be a potential cause of irreversible changes in the global climate. These concerns and discussions have been recently voiced in the *Study of Critical Environmental Problems* (SCEP, 1970) and the *Study of Man's Impact on Climate* (SMIC, 1971) and numerous other publications. However, a general conclusion on the influence of pollution on the climate is at present impossible due to the limitations in the available data and understanding. Calculations of a globally averaged radiative energy budget (Rasool and Schneider, 1971; Ensor *et al.*, 1971; and others) have been inconclusive since it has been shown that the net influence of the aerosol could be warming or cooling depending upon its properties. Also, there is considerable uncertainty in the globally averaged aerosol properties and surface reflectance. Except for those of Mitchell (1971) the predictions also fail to account for the interaction of atmospheric radiation and convective energy exchange in the atmosphere.

Another aspect of the problem of the global climate is the modification by pollutants of the temperature in an urban area. This micrometeorological question is also

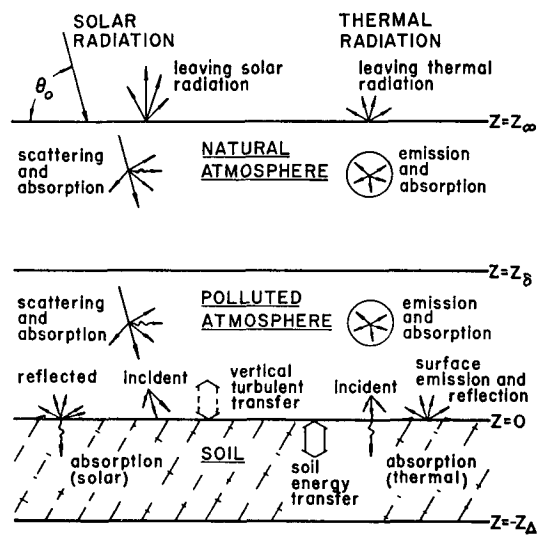

FIG. 1. Physical model for solar and atmospheric thermal radiation transfer in a polluted urban atmosphere.

[1] Current affiliation: Institut für Meteorologie, Johannes Gutenberg-Universität, Mainz, Germany.

quite difficult to answer since it involves the interaction of atmospheric radiation and atmospheric turbulence, both extremely complex phenomena. Previous attempts to couple the influences of air pollutants or aerosol hazes with the dynamics of the lower atmosphere (Atwater, 1970, 1972; Pandolfo *et al.*, 1971; Zdunkowski and Mcquage, 1972) have shown that the effects can be substantial within a period of a few days. The surface temperature has been predicted to be warmer at night and colder during the day due to infrared and solar radiation properties, respectively. However, Zdunkowski and Mcquage (1972) did not compute the solar heating caused by aerosols, Atwater (1970, 1972) did not account for vertical diffusion of pollution, and Pandolfo *et al.* (1971) treated the coupling of diffusion and the radiative effects of pollution only briefly. In this paper the influence of radiative effects of air pollution and the diffusion of pollutants are coupled, and the thermal structure is predicted by a one-dimensional transient model of the lower troposphere.

2. Analysis

a. Physical model

The physical model of the atmosphere is depicted in Fig. 1. As shown, the atmosphere-earth system is assumed to be composed of three layers: 1) the "natural" atmosphere where the atmospheric variables are considered to be time independent; 2) the "polluted" atmosphere (the planetary boundary layer) where the atmospheric variables of horizontal velocity, temperature and concentration are functions of height and time; and 3) the soil layer where the temperature is a function of depth and time. The forcing function of the model is the time-dependent solar radiation. During the day, solar radiant energy passing through natural and polluted atmospheres is depleted by absorption and scattering, and at the surface is reflected and absorbed. This absorbed energy is partially transferred to the atmosphere by turbulent convection and to the soil by conduction. The earth's surface emits energy in the form of longwave thermal radiation while the atmosphere also absorbs, emits and scatters thermal radiation. At night the emission of thermal radiation cools the atmosphere as well as the surface, and energy is transferred from the atmosphere to the surface. The physical model of the atmosphere is thus one where the atmosphere and the surface warm up during the day due to the absorption of solar radiation and cool during the night due to the emission of thermal radiation. The distribution of thermal energy in the atmosphere depends upon the turbulent vertical dispersion and the absorption of solar radiation as well as the absorption and emission of infrared radiation. The influence of air pollution is to increase the scattering and absorption of solar radiation and the absorption and emission of thermal radiation.

The atmosphere is assumed to be horizontally homogeneous and horizontal advection is neglected. This is probably valid for a region with a flat uniform terrain but, in general, would not be true for an urban area. The assumption neglects the change in the temperature structure of rural air as it is advected over a city. While this assumption can be criticized as unrealistic, it can be argued as somewhat representative of the worst possible case. Pollution episodes often occur in periods of stagnating high pressure centers with light winds. Thus, as far as large-scale processes are concerned the neglect of horizontal advection is somewhat reasonable. On a smaller scale, however, this assumption does not account for the local horizontal pollutant transport. This is probably justified for large area sources of pollution but certainly not for large point sources such as industrial smoke stacks. The main justification of the horizontal homogeneity assumption is that it permits the development of a somewhat realistic yet relatively straightforward numerical model.

With this assumption it is possible to incorporate a fairly detailed description of radiative energy transfer without involving excessive computer time. This one-dimensional model of energy transfer should therefore be considered as a first approximation, while for more realistic modeling of an urban area a two- or a three-dimensional model would be necessary. Even in a three-dimensional model the radiative transfer would probably have to be considered one-dimensional, because of excessive computer time requirements.

The horizontal homogeneity assumption implies that the mean vertical velocity vanishes everywhere. This is equivalent to neglecting any upward flow due to the growth of the urban boundary layer (a result of the fully developed or horizontal homogeneity requirement) and to neglecting any free convection pattern formed by the city.

b. Nomenclature

In order to give a brief presentation of the governing equations it is necessary to first define the following quantities:

C_n	concentration of species n
$\dot{C}_n$	volumetric mass source of species n
c_p	specific heat at constant pressure
$\mathcal{F}$	radiant flux in the z direction defined in Eq. (12)
F	unidirectional radiant flux defined in Eq. (14)
f	Coriolis parameter or Coriolis force vector
G	incident radiant energy defined in Eq. (13)
I	intensity of radiation
$I_{b\nu}$	Planck's function $\{=(2h\nu^3m^2/c^2)[\exp(h\nu/kT)-1]^{-1}\}$
K^M	momentum turbulent diffusivity
K^Θ	thermal turbulent diffusivity
K^{C_n}	mass turbulent diffusivity
k	thermal conductivity
L	latent heat of evaporation

M Halstead moisture parameter
m mass flux due to surface source
p pressure
p_ν scattering phase function
Ri Richardson number $[=(g/\Theta)(d\Theta/dz)/(dU/dz)^2]$
T temperature
t time
U mean horizontal wind speed $[=(u^2+v^2)^{\frac{1}{2}}]$
u horizontal east velocity
v horizontal north velocity
x horizontal east coordinate
y horizontal north coordinate
z vertical coordinate
z_0 roughness length
z_δ planetary boundary layer height
z_∞ top of atmosphere
α thermal diffusivity $[=k/(\rho c_p)]$
ϵ_t surface thermal emittance
Θ potential temperature $[\equiv T(p/p_0)^{R/c_p}]$, where p_0 is the surface pressure and R the gas constant
θ zenith angle
κ absorption coefficient
μ cosine of zenith angle
ρ density or reflectance
σ scattering coefficient or Stefan-Boltzmann constant
ϕ azimuthal angle

Subscripts

ν frequency
n nth species, i.e., w is water vapor and p pollutant
s solar or soil
t thermal

Superscripts

$+$ positive z direction
$-$ negative z direction

c. Basic equations

The governing equations for the model are given below. The equations state mathematically the conservation principles of momentum, energy and species and are the same set as used by previous investigators (Estoque, 1963; Sasamori, 1970; Zdunkowski and Mcquage, 1972). In order to completely formulate the problem it is necessary to specify the initial and boundary conditions, to predict the divergence of the radiative flux, and to relate the turbulent diffusivities to the other atmospheric variables.

The governing equations for the one-dimensional, transient model are as follows:

$z=z_\infty$

Natural atmosphere

u, v, Θ, C_w, C_p = constant

$z=z_\delta$

Polluted atmosphere

$$x\text{-momentum: } \frac{\partial u}{\partial t}=-\frac{1}{\rho}\frac{\partial p}{\partial x}+\frac{\partial}{\partial z}\left[K^M\frac{\partial u}{\partial z}\right]+fv \tag{1}$$

$$y\text{-momentum: } \frac{\partial v}{\partial t}=-\frac{1}{\rho}\frac{\partial p}{\partial y}+\frac{\partial}{\partial z}\left[K^M\frac{\partial v}{\partial z}\right]-fu \tag{2}$$

$$\text{energy: } \frac{\partial \Theta}{\partial t}=\frac{\partial}{\partial z}\left[K^\Theta\frac{\partial \Theta}{\partial z}\right]-\frac{1}{\rho c_p}\frac{\partial \mathcal{F}}{\partial z} \tag{3}$$

$$\text{species: } \frac{\partial C_n}{\partial t}=\frac{\partial}{\partial z}\left[K^{C_n}\frac{\partial C_n}{\partial z}\right]+\dot{C}_n \tag{4}$$

Surface $z=0$

Soil layer

$$\text{energy: } \frac{\partial T_s}{\partial t}=\alpha_s\frac{\partial^2 T_s}{\partial z^2} \tag{5}$$

$z=-z_\Delta$

T_s = constant

The boundary conditions at the top of the planetary boundary layer are specified by requiring the values of the variables to be constant, i.e.,

$$\chi(z,t)=\text{constant at } z=z_\delta, \tag{6}$$

where χ represents the horizontal east velocity u, the horizontal north velocity v, the potential temperature Θ, and the pollutant concentration C_p. This boundary condition is consistent with the notion that the large-scale weather system is slowly moving. At the bottom of the soil layer the temperature and the moisture are also taken as constant, i.e.,

$$T_s(z,t)=\text{constant},\ C_w(z,t)=\text{constant, at } z=-z_\Delta. \tag{7}$$

At the earth's surface the two velocity components are considered to vanish, i.e.,

$$u(z,t)=v(z,t)=0, \quad \text{at} \quad z=z_0. \tag{8}$$

The surface temperature is predicted by assuming that the earth's surface cannot store energy and that it is opaque to radiation. Hence, the sum of the radiative, convective and conductive fluxes must vanish; i.e.,

$$(1-\rho_s)F_s^-(0,t)+\epsilon_t F_t^-(0,t) - \epsilon_t\sigma T^4(0,t)+(k+\rho c_p K^T)\frac{\partial T}{\partial z}\bigg|_0 +\rho L K^{C_w}\frac{\partial C_w}{\partial z}\bigg|_0-k_s\frac{\partial T_s}{\partial z}\bigg|_0=0, \quad \text{at } z=0, \tag{9}$$

where $F_s^-(0,t)$ and $F_t^-(0,t)$ represent the downward directed solar and thermal fluxes, respectively. Thus, the first and second terms represent the absorption of solar and thermal radiation by the surface, respectively. The third term accounts for the emission of thermal radiation by the surface and the fourth and fifth terms represent the turbulent thermal energy flux, and the latent energy flux leaving the surface; the last term is the conductive energy flux to or from the soil. For an

urban area an artificial heat generation contribution Q_{heat} must also be included.

The surface specific humidity is prescribed by Halstead's moisture parameter (Pandolfo *et al.*, 1971) in an approximate manner by the expression

$$C_w(0,t)=MC_{sat}(0,t)+(1-M)C_w(z_1,t), \quad \text{at} \quad z=0, \quad (10)$$

where z_1 is the first grid point above the surface and C_{sat} the saturated specific humidity. The values of the parameter M range from 1 for water $[C_w(0,t)=C_{sat}]$ to 0 for dry soil $[C_w(z_1,t)-C_w(0,t)=0]$.

The surface boundary condition for the pollution concentration when a surface source is present is given by specifying the surface pollutant mass flux, m_p, i.e.,

$$m_p=-(D_p+K^{C_p})\frac{\partial C_p}{\partial z}\bigg|_0, \quad \text{at } z=0. \quad (11)$$

d. Radiation transfer model

The radiant energy flux divergence, $\partial\mathcal{F}/\partial z$, which appears in the energy equation physically represents the net loss (or gain) of radiant energy per unit of volume. The conservation of radiant energy equation can be written as

$$\frac{\partial \mathcal{F}}{\partial z}=\int_0^\infty \{\kappa_\nu[4\pi I_{b\nu}(z)-G_\nu(z)]\}d\nu, \quad (12)$$

where the spectral incident radiant energy is defined as

$$G_\nu(z)\equiv\int_0^{2\pi}\int_{-1}^{+1} I_\nu(z,\mu,\phi)d\mu d\phi, \quad (13)$$

and the radiant flux as

$$\mathcal{F}_\nu(z)\equiv F_\nu^+(z)-F_\nu^-(z)=\int_0^{2\pi}\int_{-1}^{+1} I_\nu(z,\mu,\phi)\mu d\mu d\phi. \quad (14)$$

The first term on the right-hand side of Eq. (12) represents emission and the second term accounts for absorption of radiant energy. The spectral intensity I_ν defining the radiation field is predicted from the equation of transfer in the direction μ, ϕ as (Chandrasekhar, 1960)

$$\mu\frac{\partial I_\nu(z,\mu,\phi)}{\partial z}=-[\kappa_\nu(z)+\sigma_\nu(z)]I_\nu(z,\mu,\phi)+\kappa_\nu(z)I_{b\nu}(z)$$
$$+\frac{\sigma_\nu(z)}{4\pi}\int_{\phi'=0}^{\phi'=2\pi}\int_{\mu'=-1}^{\mu'=1} p_\nu(z,\mu',\phi'\rightarrow\mu,\phi)$$
$$\times I_\nu(z,\mu',\phi')d\mu' d\phi'. \quad (15)$$

In writing this equation it was assumed that the atmosphere is in local thermodynamic equilibrium, the index of refraction is equal to unity, and the radiative transfer is quasi-steady, i.e., $(1/c)\partial/\partial t \ll \mu(\partial/\partial z)$.

The boundary conditions necessary to solve the equation of transfer (15) are the specification of the intensity at the top of the atmosphere and at the surface. At the top of the atmosphere it is assumed that the sun is the only source of radiation present and at the surface of the earth it is considered that the reflection and emission are diffuse and the radiation characteristics are known. This is written as

$$I_\nu^-(z_\infty,\mu,\phi)=F_{\infty,\nu}\delta(\mu-\mu_0)\delta(\phi-\phi_0), \quad \mu<0, \quad (16)$$

$$I_\nu^+(0,\mu,\phi)=(\rho_\nu/\pi)F_\nu^-(0)+\epsilon_\nu I_{b\nu}(0), \quad \mu>0, \quad (17)$$

where δ is the Dirac delta function.

The solution of the equation of transfer was accomplished (Bergstrom and Viskanta, 1972) by dividing the entire electromagnetic spectrum into the solar part ($0.3\ \mu m\leqslant\lambda\leqslant 4\ \mu m$) and the thermal (infrared) part ($4\ \mu m\leqslant\lambda\leqslant 100\ \mu m$). In the solar part the integro-differential equation of transfer was solved analytically using the spherical harmonics approximation. The solutions based on the P_3 approximation of the spherical harmonics method were found to be in good agreement with the results of other more detailed methods, and are discussed by Bergstrom and Viskanta (1973a).

The total radiative flux and flux divergence in the thermal spectrum were predicted by simply using the total emissivity data from Kuhn (1963) for water vapor and carbon dioxide from Shekhter (Atwater, 1970), and neglecting multiple scattering. It was also assumed that the influence of gaseous pollutants was confined to the 8–12 μm spectral region.

The spectral absorption and scattering characteristics of the pollution aerosol must be specified before solutions can be obtained. A truly accurate treatment is extremely complex and not practical because of lack of data. The absorption and scattering coefficients and the scattering distribution function were predicted using Mie electromagnetic theory by specifying the size distribution [Deirmendjian's Haze L distribution; Deirmendjian (1969)] and assuming that the aerosol is composed of absorbing (carbon-like) and non-absorbing (quartz-like) spheres. While the latter assumption can be criticized as somewhat arbitrary, the resulting absorption and extinction coefficients correspond fairly well to the bulk mean indices of refraction measured by Fisher and Hänel (Hänel, 1972) for a dry aerosol over an industrialized area. The details of the model are given by Bergstrom (1972).

e. Turbulent diffusivities and method of solution

The equations also require the specification of the turbulent diffusivities. The diffusivity for an arbitrary quantity ξ in the j direction is defined as

$$K_j^\xi\equiv-\overline{\xi' v_j'}/(\partial\bar{\xi}/\partial x_j), \quad (18)$$

where the primes represent instantaneous values and the bars time-averaged quantities. The expressions for

the diffusivities as developed by Pandolfo *et al.* (1971) from simularity theory considerations were employed. These relationships are presented in Table 1. In this study the diffusivities were assumed to be valid over the entire planetary boundary layer for simplicity. The decay of turbulence in the upper planetary boundary layer was accounted for following Blackadar (1962) and Wu (1965) by replacing the height z with a length l, where

$$l=\frac{z}{1+z/\lambda}, \tag{19}$$

and λ is a constant

The details of the finite-difference scheme are discussed elsewhere (Bergstrom and Viskanta, 1972). The implicit Crank-Nicholson method was employed with nonlinear grid spacing. A variable time step was used to keep the largest stability parameter below a certain set value. Since the solar radiation divergence was the most time-consuming calculation, longer time steps were used in this computation than for other variables, and the values then extrapolated in between computations. Each two-day simulation required approximately 5 min of a CDC 6600 computer.

3. Results and discussion

The predictions of the model were compared against measured data in order to establish some degree of its reliability. The data selected were those from the Great Plains Turbulence Study (Lettau and Davidson, 1957). The pollutant conditions studied were those for an urban summer and winter, with and without an elevated inversion. The pollution parameters varied were the amount of aerosol, the amount of absorbing aerosol, the amount of pollutant gas, and the choice of the pollutant gas. In total, 32 numerical experiments were performed (Bergstrom and Viskanta, 1972). For brevity, the only cases discussed here are those without any pollution compared to those with a 20% carbon aerosol and ethylene (C_2H_4) as the air pollutant gas. The influence of aerosol absorption and the case of sulfur dioxide (SO_2) as the absorbing gas are also briefly discussed.

TABLE 1. Eddy diffusivity correlations (after Pandolfo *et al.*, 1971).

$0\leqslant \mathrm{Ri}<\mathrm{Ri}_c$:	$K^M=K^\Theta=K^{C_w}=(kz)^2\left[\frac{\partial U}{\partial z}\right](1-3\ \mathrm{Ri})^2$
$-0.048<\mathrm{Ri}<0$:	$K^M=(kz)^2\left[\frac{\partial U}{\partial z}\right](1+3\ \mathrm{Ri})^{-2}$
	$K^\Theta=K^{C_w}=K^M/(1-\mathrm{Ri})^2$
$\mathrm{Ri}\leqslant -0.048$:	$K^\Theta=K^{C_w}=c_1 z^2\left[\left(\frac{g}{\Theta}\right)\left(\frac{\partial\Theta}{\partial z}\right)\right]^{\frac{1}{2}}$
	$K^M=\frac{c_2}{\lvert\mathrm{Ri}\rvert^{1/6}}K^\Theta$

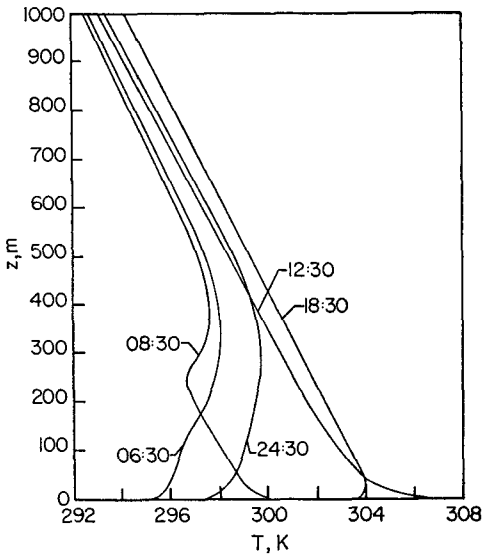

FIG. 2. Temperature profiles for the test simulation.

a. Test simulation: The O'Neill observations

The Great Plains Turbulence Study was held in 1954 and until recently was the most complete set of measurements of the temperature, velocities, humidity and radiation fluxes reported. The results of the study have been analyzed in numerous publications and both Estoque (1963) and Sasamori (1970) have simulated the conditions for the fifth observational period. Since no comparable set of data exists for an urban area this situation was chosen to test the numerical model. The input data and values for the physical constants were taken from observed or published sources.

The simulation was started at 1230 (all times LST) 24 August 1954 (which was the beginning of the data). The temperature profiles at 1230, 1830, 2430, 0630 and 0830 are illustrated in Fig. 2. These distributions show the cooling of the surface, development of the night time inversion, breakup of the inversion, and development of the superadiabatic profiles. Comparison of the predicted temperature profiles with those determined by Sasamori (1970) and those observed show relatively good agreement (Bergstrom and Viskanta, 1972, Fig. 6.2). Both analytical models predicted a surface inversion (as did Estoque, 1963) which was not observed. However, Deardorff (1967) has suggested as a possible explanation the advection of cold air during the night.

The predicted surface fluxes and those inferred by Suomi (Lettau and Davidson, 1957) are compared in Table 2. The entries show that the energy supplied by radiant flux during the day is transferred to the soil and the atmosphere, whereas at night energy is transferred from the atmosphere and soil to the surface. The agreement between the predicted and the inferred surface fluxes is fairly good. Particularly encouraging is the finding that the radiation fluxes are within 10–20% of the observed. The natural aerosol conditions were

TABLE 2. Comparison of inferred (a) [Lettau and Davidson (1957); 24–25 August 1954] and predicted (b) energy fluxes. Units: ergs cm^{-2} sec^{-1}.

Time (LST)	Net radiation (a)	Net radiation (b)	Soil conduction (a)	Soil conduction (b)	Turbulent convection (a)	Turbulent convection (b)	Latent heat transport (a)	Latent heat transport (b)
1235	-6.43×10^5	-5.32×10^5	9.45×10^4	1.71×10^5	4.32×10^5	2.995×10^5	1.10×10^5	5.45×10^4
1435	-5.14×10^5	-4.371×10^5	5.43×10^4	1.05×10^5	3.76×10^5	3.06×10^5	7.42×10^4	5.15×10^4
1635	-2.13×10^5	-1.939×10^5	-1.75×10^4	6.18×10^4	2.39×10^5	1.54×10^5	1.4×10^3	4.06×10^4
1835	5.18×10^4	4.85×10^4	-2.24×10^4	1.54×10^4	-2.94×10^4	-4.09×10^4	3.5×10^3	2.02×10^4
2035	8.26×10^4	7.72×10^4	-2.66×10^4	-2.14×10^4	-4.48×10^4	-5.95×10^4	-9.8×10^3	3.58×10^3
2235	8.26×10^4	7.56×10^4	-2.38×10^4	-1.83×10^4	-2.73×10^4	-5.92×10^4	-3.28×10^4	1.85×10^3
0035	8.40×10^4	7.44×10^4	-2.59×10^4	-1.84×10^4	-3.22×10^4	-5.64×10^4	-2.59×10^4	2.84×10^2
0235	8.12×10^4	7.28×10^4	-2.66×10^4	-2.09×10^4	-3.99×10^4	-5.08×10^4	-1.54×10^4	-1.19×10^3
0435	8.26×10^4	7.15×10^4	-2.73×10^4	-2.32×10^4	-3.29×10^4	-4.59×10^4	-2.31×10^4	-2.35×10^3
0635	2.31×10^4	3.11×10^4	-1.61×10^4	-1.73×10^4	-2.8×10^3	-3.58×10^4	-4.2×10^3	-2.72×10^3
0835	-2.63×10^5	-1.476×10^5	3.57×10^4	5.21×10^4	1.71×10^5	9.65×10^4	5.60×10^4	9.78×10^3
1035	-5.25×10^5	-4.41×10^5	7.70×10^4	1.04×10^5	3.56×10^5	2.64×10^5	9.24×10^4	3.30×10^4
1235	-6.09×10^5	-5.30×10^5	9.17×10^4	1.03×10^5	4.14×10^5	3.67×10^5	1.043×10^5	5.73×10^4

not measured and were assumed to correspond to that of high visibility (Elterman, 1970). No pollution aerosols were assumed to be present. The solar reflectance was chosen to be 0.3 and was an average of values determined in another observational period. Both the solar and thermal radiant flux are underestimated. Sasamori (1970) also underpredicted the solar flux due to the uncertainties of the atmospheric conditions and reflectance.

For the purposes of this study the present analysis has been shown to compare well with other one-dimensional studies. The advantages of this model are that a constant flux layer is not assumed and the solar radiation does not have to be known *a priori* at the surface but is computed.

b. *The urban summer*

The purpose of this experiment was to simulate a summer condition of an urban area. The same initial variables as the O'Neill study with urban values of the parameters z_0, M, Q_{heat} (artificial heat generation parameter), α_s and k_s were selected. The values for these parameters are summarized in Table 3. The general influences of these quantities on the urban surface temperature have been well documented [e.g., Pandolfo *et al.* (1971, p. 46, Fig. 3.2-1) and Atwater (1972, Figs. 1–3)] and need not be repeated here. It should be noted that Atwater (1972) concluded that the physical properties of the surface are the dominant factors in creating the urban heat island.

TABLE 3. Urban and pollution parameters.

	Urban parameters	
z_0	100 cm	Pandolfo *et al.*, 1971
M	0	Pandolfo *et al.*, 1971
Q_{heat}	-9.0923×10^4 erg cm^{-2} sec^{-1}	McElroy, 1971, and Pandolfo *et al.*, 1971
α_{soil}	2.2×10^{-2} cm^2 sec^{-1}	Pandolfo *et al.*, 1971
k_{soil}	4.598×10^5 ergs cm^{-1} sec^{-1} $(°C)^{-1}$	Pandolfo *et al.*, 1971
r_s	0.1	Ludwig *et al.*, 1969
	Pollution parameters	
pollutant source	3 μg m^{-2} sec^{-1}	Pandolfo *et al.*, 1971
z_s	0	Uthe, 1971
aerosol	20% carbon	Bergstrom, 1972
gas	ethylene	Ludwig *et al.*, 1969

The pollution parameters employed in the simulations are also shown in Table 3. The pollution source was taken to be that of an industrialized area in the Hartford, Conn., study (Pandolfo *et al.*) and was found to give reasonable pollution concentration. The pollution concentrations are presented in a companion paper (Bergstrom and Viskanta, 1973b) and were typical of a polluted urban area. Since a surface source was shown by Uthe (1971) to be approximately valid for the study of St. Louis, it was used in the simulations. The pollution aerosol composition of quartz and carbon was selected from the aerosol model from Bergstrom (1972) as previously discussed. Ethylene was at first chosen to simulate gaseous pollutants since Ludwig *et al.* (1969) considered it to be representative of a typical hydrocarbon and since it was shown to have strong absorption in the 8–12 μm range. Obviously, other individual gases such as ammonia or gas mixtures could have been used to simulate the actual polluted conditions; however, in this initial study a more detailed description of gaseous pollutants was considered to be unwarranted.

The results for the temperature distribution as a function of both height and time are shown in Fig. 3a for the simulation with nonparticipating pollutants. The temperatures are warmer at night than for the corresponding O'Neill study due to the change from a rural to an urban area. There is essentially no inversion and the warming trend during the computational period is enhanced. Temperature profiles for a simulation with radiatively participating pollutants are illustrated in Fig. 3b. Note that the general trends are the same as the first simulation but the magnitude of the temperatures is different. The difference[2] in the temperatures is

[2] The difference is defined as the quantity in the simulation with nonparticipating pollutants minus the quantities in simulation with the radiatively participating pollutants.

illustrated in Fig. 3c. As shown, the temperatures are warmer at night by a maximum of 2.2C and cooler during the day by a maximum of 0.4C. Thus, the net effect is a reduction in diurnal temperature variation of 2.6C from a total of 8–10C.

The surface solar and atmospheric radiant energy fluxes for the two experiments are presented in Table 4. It is clear from the table that the pollutants reduce the solar flux and increase the thermal flux. This indicates the reason why the surface temperature is cooler during the day and warmer during the night in the simulation with participating pollutants. The solar flux is reduced by about 10% on the first day and 20% on the second. This is well within the range of observed reduction of solar fluxes in an urban area (Peterson, 1969). The downward thermal radiation flux is increased by about 10%. However, the flux is also a function of the temperature profile and the temperatures are somewhat warmer at night and cooler during the day in Fig. 3b. The increase agrees with observations of Oke and Fuggle (1972) who measured an increase of about 10% in the downward thermal flux in Montreal, as compared to the surrounding countryside. Thus, the alterations in the radiant flux appear to be quite realistic and agree with available experimental evidence. However, it must be noted that Oke and Fuggle suggested that the increase in thermal flux could be due to the warmer temperatures and not to the pressence of pollutants.

TABLE 4. Comparison of solar flux and thermal downward flux at the surface for urban summer simulations.*

Time (LST)	Solar, $\mathcal{F}(0)$ (ergs cm^{-2} sec^{-1}) w_0	w	Thermal, $F^-(0)$ (ergs cm^{-2} sec^{-1}) w_0	w
1230	8.22×10^5	8.22×10^5	3.95×10^5	3.95×10^5
1430	7.07×10^5	7.00×10^5	4.02	4.33
1630	3.87×10^5	3.72×10^5	4.02	4.38
1830	5.37×10^4	4.91×10^4	3.95	4.34
2030			3.89	4.31
2230			3.85	4.30
2430			3.83	4.29
0230			3.81	4.28
0430			3.78	4.27
0630	5.37×10^4	4.21×10^4	3.76	4.25
0830	3.87×10^5	3.14×10^5	3.85	4.32
1030	7.07×10^5	6.09×10^5	3.96	4.43
1230	8.28×10^5	7.20×10^5	4.05	4.53
1430	7.07×10^5	5.91×10^5	4.10	4.62
1630	3.87×10^5	2.87×10^5	4.09	4.61
1830	5.37×10^4	3.65×10^4	4.02	4.51
2030			3.95	4.50
2230			3.92	4.47
2430			3.88	4.45
0230			3.85	4.43
0430			3.83	4.41
0630	5.37×10^4	3.22×10^4	3.80	4.39
0830	3.87×10^5	2.44×10^5	3.83	4.32
1030	7.07×10^5	5.07×10^5	4.00	4.54
1230	8.28×10^5	6.13×10^5	4.09	4.66

* With (w) and without (w_0) radiatively participating pollutants.

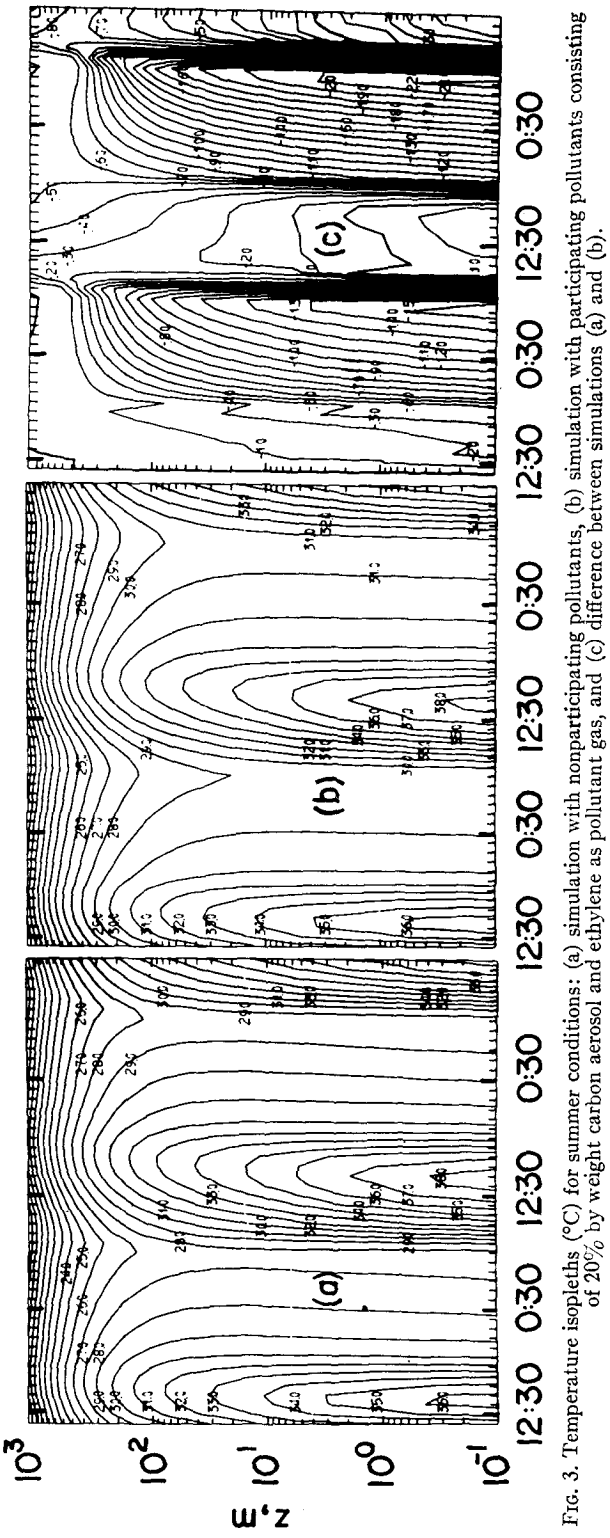

FIG. 3. Temperature isopleths (°C) for summer conditions: (a) simulation with nonparticipating pollutants, (b) simulation with participating pollutants consisting of 20% by weight carbon aerosol and ethylene as pollutant gas, and (c) difference between simulations (a) and (b).

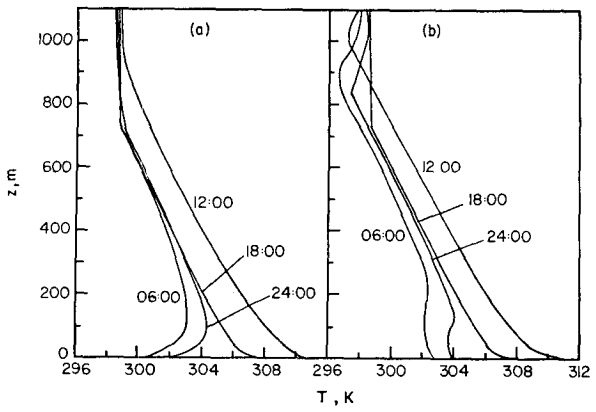

FIG. 4. Temperature profiles for summer elevated inversion conditions: (a) simulation with nonparticipating pollutants and (b) simulation with participating pollutants consisting of 20% by weight carbon aerosol and ethylene as pollutant gas.

c. *The urban summer elevated inversion*

Since pollution episodies usually occur when an elevated inversion is present, the urban summer situation was investigated with a layer of stable air[3] above 750 m. Experiments using the same starting time and velocities as the urban summer simulation showed that the stable region was destroyed by the good afternoon mixing within 1 hr. In order to investigate the effect of pollutants under inversion conditions, the simulations were started in the evening (1700) and the velocities reduced to one-fourth the values of the O'Neill data. The temperatures at 6-hr intervals are shown in Fig. 4a. As indicated, a radiative inversion develops at night due to the reduction in wind and corresponding lower diffusivities.

During the next day the mixing destroys the stable layer while the elevated stable region inhibits the upward heat flux causing the surface temperature to be greater than in the simulation without the inversion. The reduction in wind speed also tends to increase the surface temperature. This simulation is very similar to the O'Neill simulation in that a radiative inversion develops, deepens, and is destroyed. The destruction of the surface stable region has occurred by 1200 and the elevated stable region has been moved upward to about 900 m.

As shown in Fig. 4b the radiatively participating pollutants have a pronounced effect on the temperature distribution. The surface inversion does not develop since the increase in thermal radiation increases the surface temperature about 2C. There is cooling at two different levels: 1) at the base of the nighttime stable layer at 100 m, and 2) at 650 m at the height of the elevated inversion. Both of these colder regions result from the thermal radiation cooling by the pollutants which are trapped beneath the stable regions. The temperature profiles show that a weaker elevated inversion forms at about 100 m instead of the radiative surface inversion. This weak elevated inversion has also been predicted by Atwater (1970) and Pandolfo *et al.* (1971). The inversion moves upward and weakens further during the early morning hours. The base of the stable region at 750 m also cools and is moved upward during the night.

The changes in the surface radiative flux for these two situations are similar to simulations previously discussed and therefore are not presented. The downward thermal radiative fluxes were larger while the solar radiative flux was 10–20% smaller in the simulation where the radiative effects of pollution were considered.

d. *The urban winter*

In order to evaluate the influence of the change in the season on the influence of air pollution on the thermal structure and pollutant dispersion an urban winter condition was simulated. The only major changes are in the solar declination, initial temperature and humidity, and starting time. The solar declination is that of Nebraska in January. The initial temperature profile is presumed adiabatic at 1700 with a surface temperature of about 15C. The free atmosphere conditions were taken from Atwater (1970) and the urban and pollution parameters are the same as before.

The temperature for the experiment without radiatively participating pollutants is shown in Fig. 5a. The difference between day and night temperatures is only 4C which is less than that during the summer. This is in agreement with other investigators (Pandolfo *et al.*). The results for the simulation with participating pollutants are illustrated in Fig. 5b and the difference in Fig. 5c. During the first night and next day the temperature differences in Fig. 5b are warmer than in Fig. 5a near the surface at night, the maximum being −1.6C, and the difference decreasing during the day to −0.1C. The cycle is repeated during the second day as the temperatures are 0.2C smaller during the second day. At 2000 and an altitude of about 600 m the temperatures in Fig. 5b are lower than those in 5a due to the infrared cooling by the pollutants.

The surface fluxes for the solar radiation and the downward thermal radiation are shown in Table 5. The thermal radiation flux for the simulation with radiatively participating pollutants increases quite rapidly and is 8% higher within 2 hr. The average increase of thermal radiation flux is about 20% and solar radiation is reduced to about 10–30%. This decrease in the solar flux is larger than the summer simulations and is due to the fact that the average solar elevation angle is lower in the winter. The larger increase in the thermal radiation flux is apparently due to the lower specific humidities in the winter situation. The rate of increase of the

[3] Since the vertical velocity was assumed to be zero it was not possible to include a subsidence production term to maintain the inversion. Thus, this situation physically represents an elevated inversion which has been produced and the production process ceased.

thermal radiation flux slows down as the spectral region becomes relatively opaque.

Simulations were performed for the winter conditions with an elevated inversion (Bergstrom and Viskanta, 1972); however, for the sake of brevity the results are not included here. As in the summer case, the strong radiational cooling resulted in an upward motion of the stable region. The potential for the modification of a stable region is then clearly indicated.

e. Effects of the choice of gaseous pollutant

As explained earlier, ethylene was chosen since it can be considered to be a representative hydrocarbon and is a strong absorber in the 8–12 μm region. This choice, however, may be criticized as an oversimplification of an urban atmosphere. Therefore, to investigate the sensitivity of the predicted effects to the choice of the gaseous pollutant, sulfur dioxide was considered, using the SO_2 emittance data of Chan and Tien (1971). The difference between the simulation without radiatively participating pollutants and the simulation with SO_2 and a 20% carbon aerosol for the situation of an urban summer with an elevated stable layer is shown in Fig. 6. As shown, the influences due to the gaseous pollutant decreased since SO_2 is a weaker absorber than C_2H_4. The surface temperatures are 0.75C warmer during the second night and the stable layer is moved slightly upward. However, the infrared cooling is not large enough to form a noticeable elevated inversion at 100 m.

TABLE 5. Comparison of the solar radiant flux and the downward thermal flux for urban winter conditions.*

Time (LST)	Solar, $\mathcal{F}(0)$ (ergs cm^{-2} sec^{-1}) w_0	w	Thermal, $F_t^-(0)$ (ergs cm^{-2} sec^{-1}) w_0	w
1700	4.869×10^4	4.87×10^4	2.76×10^5	2.76×10^5
1900			2.74	3.13
2100			2.72	3.19
2300			2.70	3.22
0100			2.69	3.24
0300			2.68	3.24
0500			2.67	3.25
0700			2.67	3.25
0900	4.879×10^4	3.92×10^4	2.66	3.25
1100	2.738×10^5	2.18×10^5	2.71	3.29
1300	3.838×10^5	3.08×10^5	2.75	3.38
1500	2.738×10^5	2.07×10^5	2.77	3.35
1700	4.879×10^4	3.56×10^4	2.74	3.34
1900			2.71	3.33
2100			2.70	3.32
2300			2.69	3.32
0100			2.68	3.31
0300			2.67	3.31
0500			2.66	3.30
0700			2.65	3.30
0900	4.879×10^4	2.99×10^4	2.65	3.30
1100	2.738×10^5	1.64×10^5	2.69	3.33
1300	3.837×10^5	2.37×10^5	2.72	3.36
1500	2.738×10^5	1.57×10^5	2.73	3.38
1700	4.879×10^4	2.75×10^5	2.71	3.37

* With (w) and without (w_0) radiatively participating pollutants.

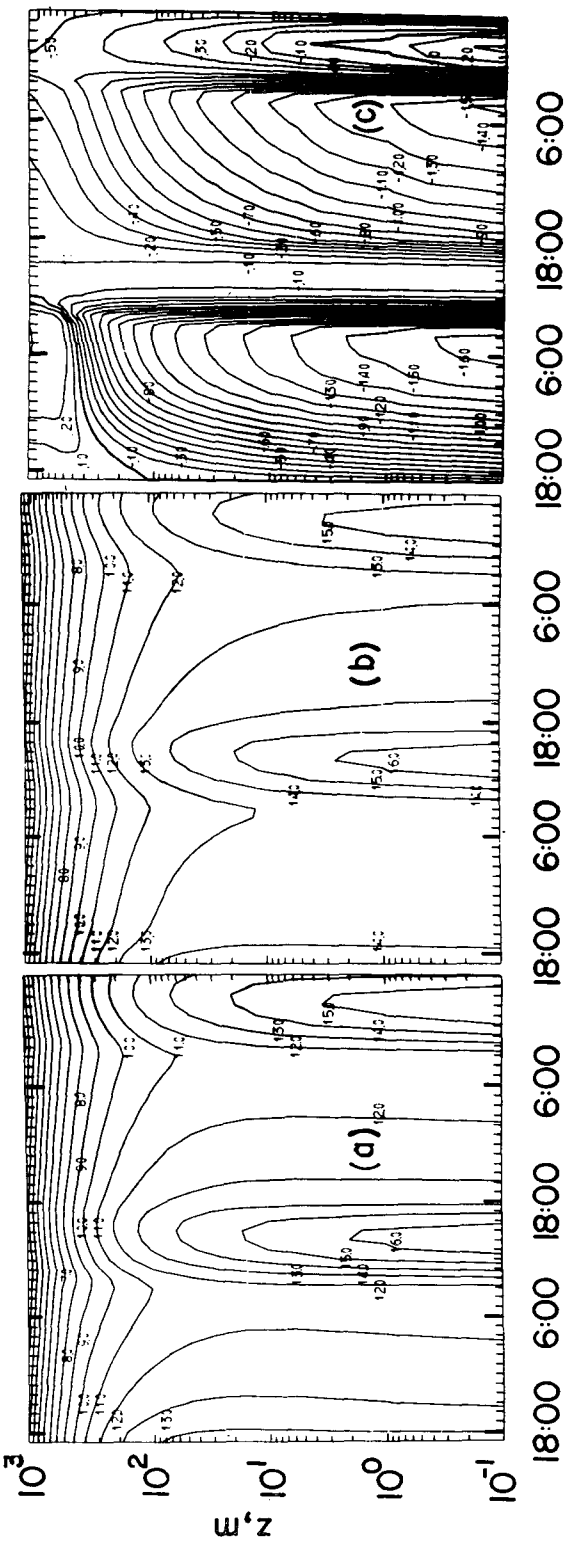

FIG. 5. As in Fig. 3 except for winter conditions.

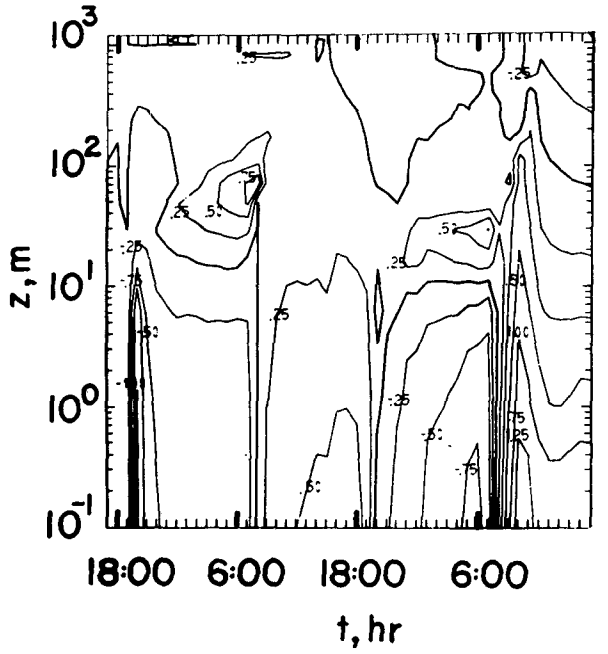

FIG. 6. Temperature difference (simulation with nonparticipating pollutants minus simulation with participating pollutants consisting of 20% by weight carbon aerosol and sulfur dioxide as pollutant gas) isopleths (°C) for summer elevated inversion conditions.

Thus, sulfur dioxide has the same qualitative effects as ethylene and only the magnitude of the results is altered. This finding is quite significant since a high concentration of SO_2 beneath stable regions is often observed (Hoffert, 1972). However, it should be mentioned that while the concentrations of the gaseous pollutant are reasonable for hydrocarbons (Bergstrom and Viskanta, 1972) they are somewhat too high for SO_2.

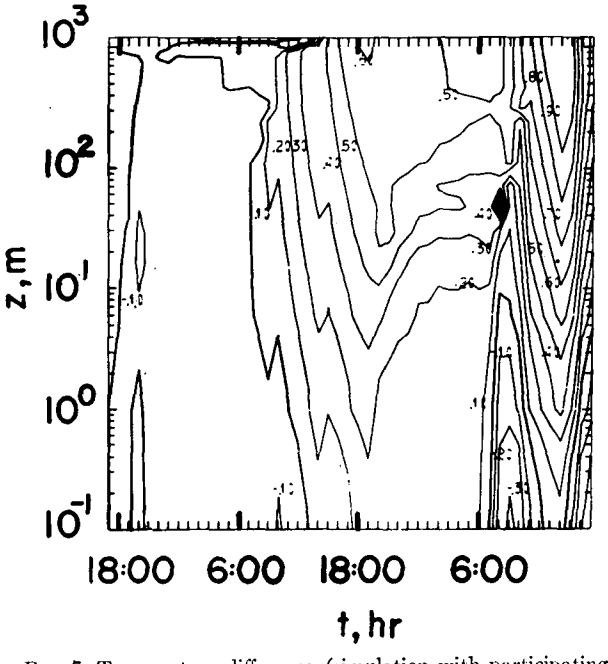

FIG. 7. Temperature difference (simulation with participating pollutants consisting of 20% by weight carbon aerosol and ethylene as pollutant gas minus simulation with non-absorbing aerosol and ethylene as pollutant gas) isopleths (°C) for summer elevated inversion conditions.

f. Effect of decreasing aerosol absorption

Since the radiative properties of aerosols are not well known, the amount of absorbing particles in the aerosol was varied to determine their relative influence on the results. In this simulation it was assumed that the aerosol was nonabsorbing (i.e., only scattering). The effects due to aerosol absorption are most clearly shown in Fig. 7. The temperatures for a non-absorbing aerosol are lower than those for an absorbing aerosol at altitudes higher than 10 m. This is due to the solar heating of the aerosols and is as large as 0.9C. The surface temperatures during the day are somewhat higher for the simulation with the non-absorbing aerosol since a larger fraction of the incident solar radiation reaches the surface.

g. Summary of surface temperature differences

The differences in the surface temperatures for the urban summer simulations in the absence of an elevated

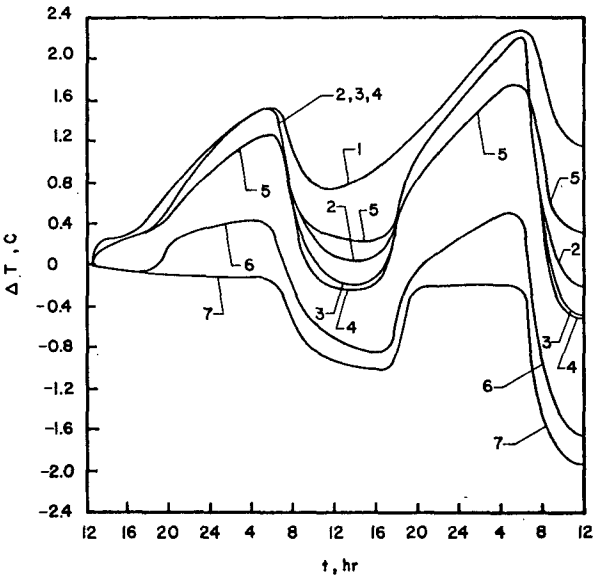

FIG. 8. Surface temperature difference (simulation with nonparticipating pollutants minus simulation with participating pollutants) for summer conditions:

Curve	Pollutant gas	Aerosol	Surface pollution mass flux (μg cm^{-2} sec^{-1})
1	C_2H_4	nonparticipating	1
2	C_2H_4	non-absorbing	1
3	C_2H_4	20% carbon	1
4	C_2H_4	30% carbon	1
5	C_2H_4	20% carbon	1/3
6	SO_2	20% carbon	1
7	nonparticipating	30% carbon	1

stable layer are shown in Fig. 8. For the conditions with C_2H_4 alone the temperature is 1.5C warmer during the first night, reduces to 0.8C warmer during the day, and rises to 2.3C warmer during the next night. The simulation with only aerosol is essentially the same as the one with nonparticipating pollutants during the first night, 1C cooler during the day, slightly cooler during the next night, and 2C cooler during the last day. This shows quite clearly the warming tendency of the gas (infrared properties) and the cooling tendency of the aerosol (solar properties). It should be mentioned that considerations of the influence of aerosols on the temperature of the atmosphere have indicated that for most combinations of aerosol properties and surface reflectance the effect of increasing aerosol is one of cooling the atmosphere. However, there are combinations of aerosol absorption and surface reflection characteristics for which the effect of the aerosol is that of warming the earth-atmosphere system (Yamamoto and Tanaka, 1972); thus, since the absorption properties of the aerosols are not well known this issue is still in doubt.

The other temperature differences lie between these two extremes. For the simulation with both ethylene and aerosol it is almost as warm during the night as with ethylene alone, but the surface is cooler during the day. The reduction of the source strength by one-third shows that temperature differences are reduced but not proportionately. In the simulation with SO_2 the surface is cooler than in the simulations with C_2H_2 due to the reduction in absorptance but the influence of SO_2 is still apparent. The effect of increased absorption by the aerosol increases the cooling of the surface (compare curves 3 and 4). Thus, in these simulations the aerosol and the gas had somewhat compensating effects. However, whether the effects cancel or one dominates over the other is clearly a function of the radiative properties of the gaseous and particulate pollutants and the atmospheric conditions.

4. Conclusions

From the results obtained it was concluded that:

1) The aerosols reduced the surface temperature by decreasing the solar radiation flux from 10–20% at the surface under the specific conditions studied. As a result of this reduction in the solar flux, the largest surface temperature decrease was 2C in two days.

2) The additional solar heating due to the aerosols increased the atmospheric temperature above the surface. The maximum temperature difference observed was 0.9C between simulations with a non-absorbing aerosol and those with an aerosol containing 20% carbon particles by weight.

3) The effect of the pollutant aerosol on the temperatures was greater in the summer than in the winter simulations due to the larger solar radiant energy fluxes incident on the earth's surface during the summer.

4) Absorption and emission of thermal radiation by pollutants raised the nocturnal surface temperature by increasing the downward thermal radiation flux. The maximum predicted temperature change was 3C. The increase in the thermal radiative flux was larger in the winter than in the summer simulations presumably due to smaller water vapor concentration in the atmosphere during the winter.

5) When the pollutant concentration distribution was nonuniform the radiational cooling was enhanced. This cooling modified both the nocturnal surface and elevated stable layers. In one of the simulations a weak inversion was created at an altitude of about 100 m.

6) The infrared cooling significantly altered the elevated stable region by transferring energy from the stable layer and moving it upward.

7) In the simulations reported the net influence of the particulates was to decrease the temperature of the atmosphere-earth system, whereas the influence of absorption and emission of thermal radiation by gases was to increase the system temperature. The gaseous and particulate pollutants thus had opposite and partially compensating effects.

Acknowledgments. This research was supported, in part, by the Division of Meteorology, Environmental Protection Agency, under Public Health Service Grant APO 1278-01 and Environmental Protection Agency Grant R801102. The National Science Foundation provided support to one of the authors (R.W.B.) in a form of a traineeship. Computing facilities were made available by Purdue University Computer Center and the National Center for Atmospheric Research which is sponsored by the National Science Foundation.

The authors wish to express their appreciation to Prof. G. M. Jurica, Department of Geosciences, Purdue University, for his interest and to Prof. K. Bullrich, Institut für Meteorologie, Johannes Gutenberg-Universität, for his valuable comments during the preparation of this paper.

REFERENCES

Atwater, M. A., 1970: Investigation of the radiative balance for polluted layers of the urban environment. Ph.D. dissertation, New York University.

——, 1972: Thermal effects of urbanization and industrialization in the boundary layer: A numerical study. *Boundary-Layer Meteor.*, **3**, 229–245.

Bergstrom, R. W., 1972: Prediction of the spectral absorption and extinction coefficients of an urban air pollution aerosol model. *Atmos. Environ.*, **6**, 247–258.

——, and R. Viskanta, 1972: Theoretical study of the thermal structure and dispersion in polluted urban atmospheres. Heat Transfer Laboratory Report, School of Mechanical Engineering, Purdue University.

——, and ——, 1973a: Prediction of the solar radiant flux and heating rates in a polluted atmosphere. *Tellus* (in press).

——, and ——, 1973b: Modeling of the effects of gaseous and particulate pollutants in the urban atmosphere. Part II: Pollution dispersion. *J. Appl. Meteor.*, **12**, 913–918.

Blackadar, A. K., 1962: The vertical distribution of wind and

turbulent exchange in a neutral atmosphere. *J. Geophys. Res.*, **67**, 3095–3102.

Chan, S. H., and C. L. Tien, 1971: Infrared radiation properties of sulfur dioxide. *J. Heat Transfer*, **93**, 172–178.

Chandrasekhar, S., 1960: *Radiative Transfer*. New York, Dover, 8–14.

Deardorff, J. W., 1967: Empirical dependence of the eddy coefficient for heat upon stability above the lowest 50 m. *J. Appl. Meteor.*, **6**, 631–643.

Deirmendjian, D., 1969: *Electromagnetic Scattering on Spherical Polydispersions*. Elsevier, New York, 77–83.

Elterman, L., 1970: Vertical-attenuation model with eight surface meteorological ranges 2 to 13 kilometers. Rept. AFCRL-70-0200, Air Force Cambridge Research Laboratories, Bedford, Mass.

Ensor, D. S., W. M. Porch, J. J. Pilat and R. J. Charlson, 1971: Influence of the atmospheric aerosol on albedo. *J. Appl. Meteor.*, **10**, 1303–1306.

Estoque, M. A., 1963: A numerical model of atmospheric boundary layer. *J. Geophys. Res.*, **68**, 1103–1113.

Hänel, G., 1972: Computation of the extinction of visible radiation by atmospheric particles as a function of relative humidity, based on measured properties. *Aerosol Sci.*, **3**, 377–386.

Hoffert, M. I., 1972: Atmospheric transport, dispersion, and chemical reactions in air pollution: A review. *AIAA Journal*, **10**, 377–387.

Kuhn, P. M., 1963: Radiometersonde observations of infrared flux emissivity of water vapor. *J. Appl. Meteor.*, **2**, 368–378.

Lettau, H. H., and B. Davidson, 1957: *Exploring the Atmosphere's First Mile*, Vols. 1 and 2. New York, Pergamon Press.

Ludwig, C. B., R. Bartle and M. Griggs, 1969: Study of air pollution detection by remote sensors. Rept. NASA-CR-1380, Washington, D.C.

McElroy, J. L., 1971: An experimental and numerical investigation of the nocturnal heat-island over Columbus, Ohio. Ph.D. thesis, Pennsylvania State University.

Mitchell, J. M., 1971: The effect of atmospheric aerosols on climate with special reference to temperature near the earth's surface. *J. Appl. Meteor.*, **10**, 703–714.

Oke, T. R., and R. F. Fuggle, 1972: Comparison of urban/rural counter and net radiation at night. *Boundary-Layer Meteor.*, **2**, 290–308.

Pandolfo, J. P., M. A. Atwater and G. E. Anderson, 1971: Prediction by numerical models of transport and diffusion in an urban boundary layer. Final Report, Contract 4082, The Center for the Environment and Man, Inc., Hartford, Conn.

Peterson, J. T., 1969: *The Climate of Cities: A Survey of Recent Literature*. U. S. Public Health Service, NAPCA Publ. No. AP-59, Washington, D.C.

Rasool, S. I., and S. H. Schneider, 1971: Atmospheric carbon dioxide and aerosols: Effects of large increases on global climate. *Science*, **173**, 138–141.

Sasamori, T., 1970: A numerical study of atmospheric and soil boundary layers. *J. Atmos. Sci.*, **27**, 1122–1137.

SCEP: *Man's Impact on the Global Environment: Assessments and Recommendations for Action*, 1970: Cambridge, Mass., MIT Press, 319 pp.

SMIC: *Inadvertent Climate Modification: Study of Man's Impact on Climate* (SMIC), 1971: Cambridge, Mass., MIT Press, 308 pp.

Uthe, E. E., 1971: Lidar observations of particulate distributions over extended areas. *Proceedings of the Joint Conference on Sensing of Environmental Pollutants*. AIAA Paper No. 71-1055, Amer. Inst. Aeronaut. Astronaut., New York.

Wu, S. S., 1965: A study of heat transfer coefficients in the lowest 400 meters of the atmosphere. *J. Geophys. Res.*, **70**, 1801–1807.

Yamamoto, G., and M. Tanaka, 1972: Increase of global albedo due to air pollution. *J. Atmos. Sci.*, **29**, 1405–1412.

Zdunkowski, W. G., and N. D. Mcquage, 1972: Short-term effects of aerosol on the layer near the ground in a cloudless atmosphere. *Tellus*, **24**, 237–254.